Time-dependent behaviours of railway prestressed concrete sleepers in a track system

Li, Dan; Kaewunruen, Sakdirat; You, Ruilin

DOI:
10.1016/j.engfailanal.2021.105500

Document Version
Peer reviewed version

Citation for published version (Harvard):
Li, D, Kaewunruen, S & You, R 2021, 'Time-dependent behaviours of railway prestressed concrete sleepers in a track system', *Engineering Failure Analysis*, vol. 127, 105500. https://doi.org/10.1016/j.engfailanal.2021.105500

Time-dependent behaviours of railway prestressed concrete sleepers in a track system

Dan Li[1,2], Sakdirat Kaewunruen[1,2*], Ruilin You[3]

[1] Department of Civil Engineering, School of Engineering, University of Birmingham, Birmingham B15 2TT, United Kingdom

[2] TOFU Lab (Track engineering and Operations for Future Uncertainties), School of Engineering, University of Birmingham, Birmingham B15 2TT, United Kingdom

[3] Railway Engineering Institute, China Academy of Railway Sciences, Beijing 100081, China

*** Correspondence:**
Sakdirat Kaewunruen
S.Kaewunruen@bham.ac.uk

Abstract

The main functions of railway sleepers are: (i) to safely transfer loads from wheel axles to foundation; (ii) to secure both rails ensuring correct track gauge at all time; and, (iii) to restrain movements of rails to control longitudinal creeps. In reality, railway industry can experience costly problems of railseat twists and tight gauges, for instance, due to time-dependent actions and poor workmanship. These problems prevent trains to navigate over tracks safely, effectively and quietly. They require additional, expensive maintenance activities much more frequently over time such as rail renewal, rail reprofiling/grinding, rail pad replacement, curve lubrication adjustment, etc. On this ground, it is very important to maintain the geometry and topological/dimensional stability of railway sleepers. The long-term geometric performance of sleepers can be significantly influenced by time-dependent actions and behaviours. The creep and shrinkage in prestressed concrete sleepers result in internal actions that is led to geometric deformation, which change the rail gauge and influence the safety and reliability of track components. Time-dependent behaviours also lead to increased complex internal stresses, which can cause cracking on prestressed concrete railway sleepers. The cracks stemming from creep and shrinkage can be observed in real life, at a certain time after construction, along the sleepers and near the fasteners such as anchorage, bolt holes, and web openings. In this study, unprecedented experimental and numerical investigations are conducted to evaluate time-dependent behaviours of full-scale prestressed concrete sleepers. An empirical calculation method is also introduced and the empirical results are compared with both experimental and numerical results. Insights into creep and shrinkage effects are highlighted in order to essentially aid predictive and preventative track maintenance, supporting the effective and efficient decision making of both (i) engineers and manufacturers and (ii) infrastructure managers and owners.

Keywords: prestressed concrete sleeper, creep, shrinkage, time-dependent behaviour, finite element method (FEM), numerical analysis, experiment, Eurocode

1 Introduction

Railway transportation is believed to be the safest transportation system for both passengers and goods and provides a safe, economical, and comfortable ride. Ballast railway track is the most common railway track structure used around the world. Typical ballasted railway track can be categorized into superstructure and substructure, as shown in **Figure 1**. The superstructure consists of rails, rail pads, prestressed concrete sleepers, and fastening systems. The substructure includes ballast, sub-ballast, and formation. It is important for both the superstructure and sub-structure to ensure the safety and comfort of the ride. The structural element that distributes vertical loads from rails to the substructure is the sleeper. Traditional railway sleepers can be manufactured from timber, concrete, steel, and any other engineered materials. Prestressed concrete sleepers are the most popular type in railway track around world because of its structural performance [**1-20**]. The main functions of sleepers are: to maintain rail gauge; to transfer and distribute vertical loads from rails to the underlying ballast bed; to restrain longitudinal, lateral, or vertical movement; and to hold and support rails [**21**].

Long-term performance of prestressed concrete sleepers can be influenced by many factors, such as deterioration, cracking from dynamic loads, fatigue, and environmental or chemical degradation [**22, 23**]. Sadeghi, J evaluated railway sleepers for its sufficient strength to sustain the environmental and traffic loads. Improvements by the incorporation of long-term effect were suggested in railway sleeper design [24]. Time-dependent behaviour can also significantly influence long-term performance of prestressed concrete. Creep and shrinkage can cause cracking of railway sleepers due to loss of prestress, deterioration, and increasement of internal pressure, which reduces the service life.

Creep and shrinkage of concrete were discovered in the early 20th century and have many very complex influential factors. Creep is the increasement of strain over time when the concrete structure is loaded. Shrinkage is the volume of concrete structure being reduced due to loss of water [**25**]. In recent decades, many researchers have tried to investigate mechanisms of creep and shrinkage, but they still cannot be fully understood.

The most important aspects to investigate when it comes to creep and shrinkage are material and structural analysis. In terms of material, researchers are trying to find more accurate predict model. In structural terms, the effect of creep and shrinkage will be studied. A number of experiments has been conducted to study creep and shrinkage in recent decades. There has been an improvement in the theoretical prediction and the analysis of the effects of creep and shrinkage. Presently, various design codes are predicting time-dependent behaviour such as Eurocode 2, ACI, and the Australian Standard. However, each code considering different parameters focuses on regional situation.

Investigators usually believe that creep and shrinkage have significant effects on long-span concrete structures. Most research on creep and shrinkage has focused on prestressed concrete bridge girders. W. He [**26**] stated creep and shrinkage affect camber development in prestressed bridge girders. Byle et al [**27**] monitored the long-term deformation of pretensioned high performance concrete bridge girders. Beam cambers and deflections, concrete strains, and concrete temperatures were monitored on girders in the bridge to estimate long-term behaviour. The analytical time-step method was used to predict time-dependent behaviour. A multi-scale method was utilized by Lopez [**28**] to investigate time-dependent deformation of prestressed concrete girders.

However, few researchers investigate time-dependent behaviour of prestressed concrete railway sleepers. The design process and effect factors are considered very different from prestressed concrete girders. Therefore, time-dependent behaviour of railway sleeper cannot be analysed like bridge girders.

Prestressed concrete sleeper is a very important component of railway track systems. As a prestressed concrete structure, the performance can be influenced by time-dependent behaviour. In the long-term, the deformation due to time-dependent behaviour can induce rail change. This deformation also leads to loss of prestress and reduces the capacity of concrete. Structural damages occur, such as cracks, which are the warning signs of structural failure.

This study focuses on deformation due to time-dependent behaviour because the critical dimension of railway sleepers can be significantly affected by creep and shrinkage. In this paper, a numerical study is rigorously executed to comprehensively evaluate time-dependent deformation on prestressed concrete sleepers. Experimental studies of reliability concepts for the time-dependent deformation are presented. The prediction concept based on Eurocode 2 is introduced as a method of theoretical analysis. The research also carries out statistical and probabilistic studies to investigate time-dependent behaviour.

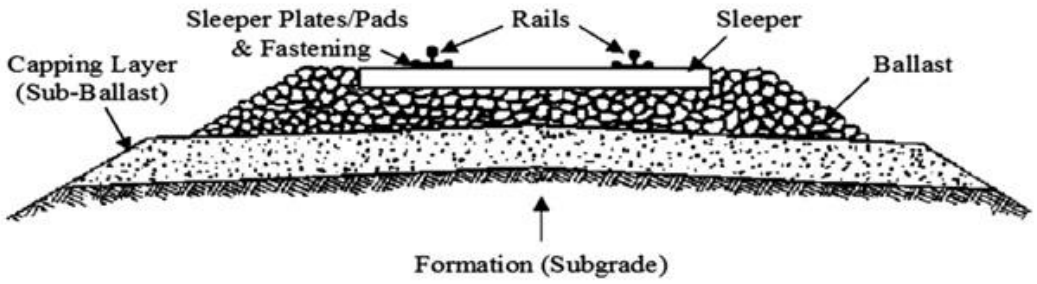

Figure 1. Ballasted railway track structure

2 Theoretical time-dependent behaviour prediction method

Eurocode 2 [**29**] describes prediction methods of creep and shrinkage, which are utilised to calculate the theoretical results of creep and shrinkage.

2.1 Creep

The total creep strain $\varepsilon_{cc}(t, t_0)$ of concrete due to the constant compressive stress of σ_c applied at the concrete age of t_0 is given by:

$$\boldsymbol{\varepsilon_{cc}(t, t_0) = \varphi(t, t_0) \times \frac{\sigma_c}{E_c}} \quad (1)$$

where:

$\varphi(t, t_0)$ is the final creep coefficient;

σ_c is the compressive stress.

E_c is the tangent modulus.

$$\boldsymbol{\varphi(t, t_0) = \varphi_{RH} \times \frac{16.8}{\sqrt{f_{cm}}} \times \frac{1}{(0.1+t_0^{0.20})}} \quad (2)$$

$$\boldsymbol{\varphi_{RH} = 1 + \frac{1-0.01\times RH}{0.1+h_0^{0.333}}, f_{cm} \leq 35MPa} \quad (3)$$

$$\boldsymbol{\varphi_{RH} = \left(1 + \frac{1-0.01\times RH}{0.1+h_0^{0.333}}\alpha_1\right)\alpha_2, f_{cm} > 35MPa} \quad (4)$$

$$\boldsymbol{\alpha_1 = \left(\frac{35}{f_{cm}}\right)^{0.7}, \alpha_2 = \left(\frac{35}{f_{cm}}\right)^{0.2} f_{cm} = f_{ck} + 8MPa} \quad (5)$$

$$\boldsymbol{t_0 = t_{0,T}\left(\frac{9}{2+t_{0,T}^{1.2}}\right)^{\alpha} \geq 0.5, \alpha = \{-1(S), 0(N), 1(R)\}} \quad (6)$$

where:

φ_{RH} is the relative humidity coefficient.

RH is relative humidity in percentage;

h_0 is the ratio of cross-sectional area and perimeter of the member in contact with the atmosphere, $h_0 = 2A_c/u$;

S, R and N refer to different classes of cement.

2.2 Shrinkage

The total shrinkage strain ε_{cs} can be given by:

$$\boldsymbol{\varepsilon_{cs} = \varepsilon_{ds} + \varepsilon_{as}} \quad (7)$$

where:

ε_{ds} is drying shrinkage strain; ε_{as} is autogenous shrinkage strain.

The drying shrinkage strain ε_{ds} can be estimated by:

$$\boldsymbol{\varepsilon_{ds} = \beta_{ds}(t, t_0) \times \varepsilon_{cd0} \times k_h} \quad (8)$$

$$\boldsymbol{\varepsilon_{cd0} = 0.85[(220 + 110\alpha_{ds1}) \times \exp(-\alpha_{sd2} \times 0.1 f_{cm})] \times 1.55[1 - (0.01RH)^3]10^6} \quad (9)$$

$$\boldsymbol{\beta_{ds}(t, t_0) = \frac{(t-t_s)}{(t-t_s)+0.04\sqrt{h_0^3}}} \quad (10)$$

where:

k_h is coefficient which depends on the national size h_0;

RH is relative humidity in percentage;

h_0 = $2A_c/u$ in mm, A_c is cross sectional area, u is the perimeter of the member in contact with the atmosphere;

The values of parameter α_{ds1} and α_{ds2} as a function of the type of cement are shown as **Table 2**.

Cement type	α_{ds1}	α_{ds2}
S	3	0.13
N	4	0.12
R	6	0.11

Table 2. Cement type and coefficient

The autogenous shrinkage strain ε_{as} can be calculated from:

$$\boldsymbol{\varepsilon_{as} = \beta_{as}(t) \times \varepsilon_{ca}(\infty)} \quad (11)$$

$$\boldsymbol{\varepsilon_{ca}(\infty) = 2.5 \times (f_{ck} - 10) \times 10^{-6}} \quad (12)$$

$$\boldsymbol{\beta_{as}(t) = 1 - \exp(-0.2t^{0.5})} \quad (13)$$

3 Type III prestressed concrete sleeper details

In this study, the 2600 mm long Chinese Type III prestressed concrete sleeper are analysed. The geometric details of the sleeper are shown in **Figure 2**. Dimension information for the selected prestressed concrete sleeper is shown below:

(a) Track gauge: 1435 mm;
(b) Concrete strength class: 42.5
(c) Distance between rail seats: 1818 mm

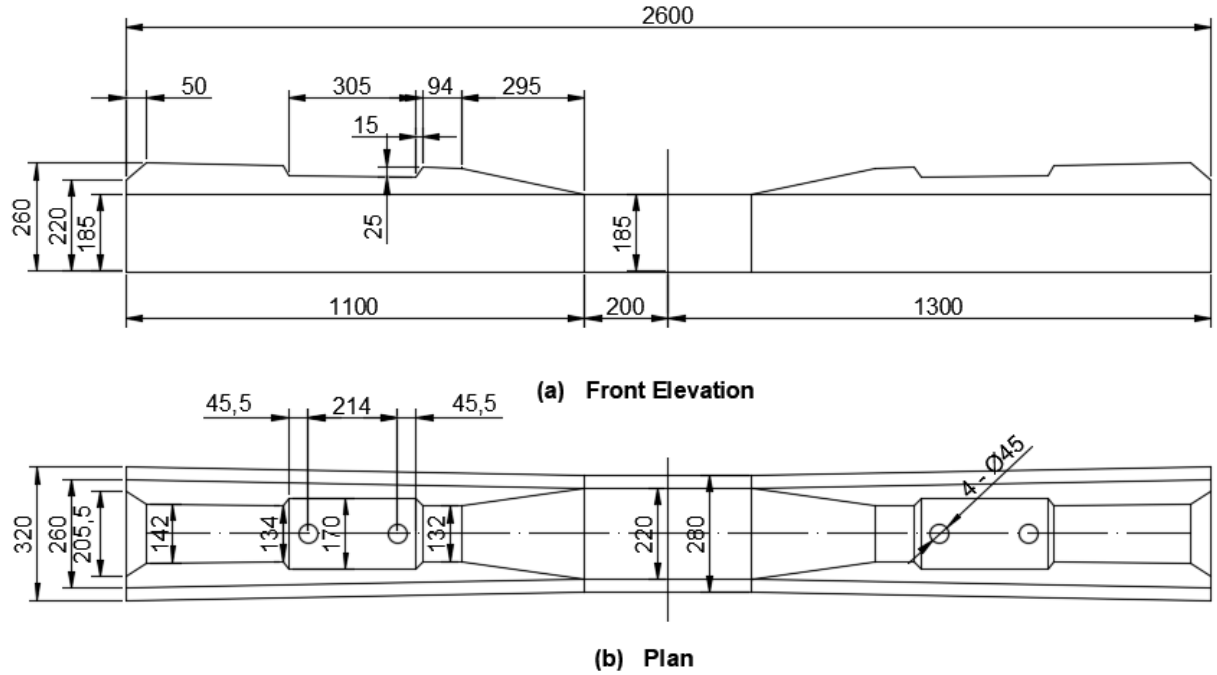

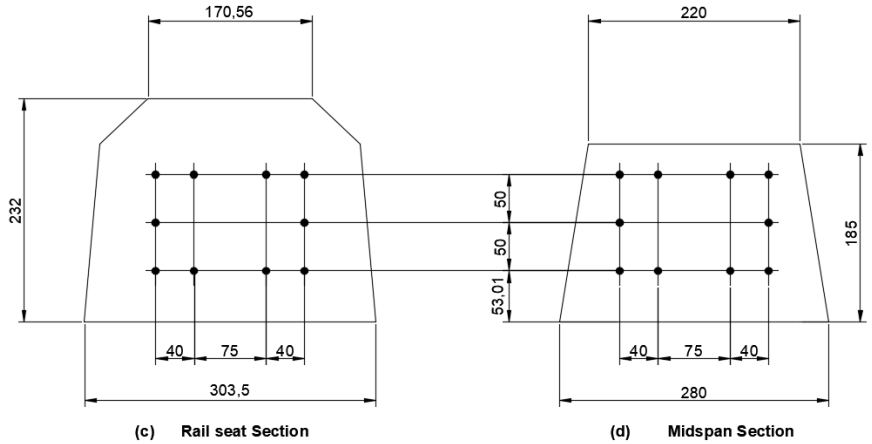

145

146 **Figure 2.** Chinese Type III prestressed concrete sleeper geometric details

147

Cement type	Basic variables	Value
Concrete properties	Mean compressive strength	65Mpa
	Modulus of elasticity	33Gpa
	Yield strength	1570Mpa
	Modulus of elasticity	200Gpa

148 **Table 3.** Material properties

149

150

151 ## 4 Finite element modelling

152 ### 4.1 Finite element model details

153 The finite element models in this paper are developed by Ansys Workbench. The model consists of
154 three parts: sleeper, ballast, and tendons. The finite element model is shown in **Figure 3**. In this research,
155 concrete and ballast (block) are modelled as solid elements. Prestressed tendons are modelled as beam
156 elements. In this FE model, concrete, prestressed tendons, and ballast are assumed to have perfect
157 contact. The material parameters of FEM are shown in **Table 4**.

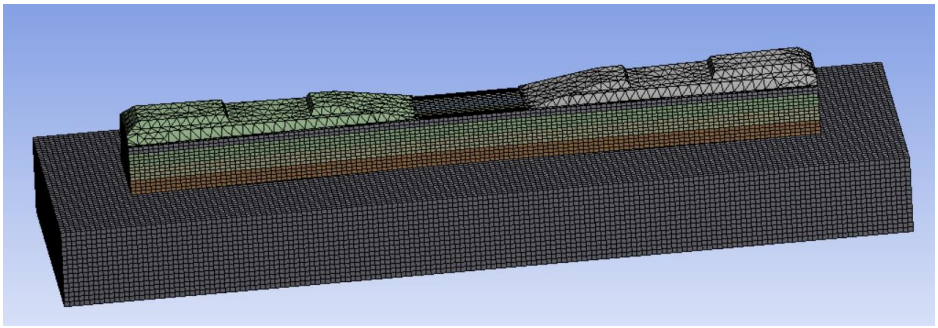

158

159 **Figure 3.** Finite element model of Chinese Type III prestressed concrete sleeper

Parts	Modulus of elasticity	Density	Poisson's ratio
	(Mpa)	(kg/m^3)	
Sleeper	33000	2400	0.23
Ballast	33000	2400	0.30
Tentons	200000	9800	0.30

Table 4. Material parameters of FEM

4.2 Element types, boundary conditions and loading

In total, the model consists of 33921 nodes and 12246 elements, with most of these elements being 10-node tetrahedron elements. In the model, the boundary conditions are No Separation, where the concrete, prestressing tendons, and ballast are assumed to be well adhered. The bottom interface of ballast is set as fixed support. In this study, the external loads are not considered for time-dependent behaviour. Therefore, the Standard Earth Gravity is applied at the FEM. The Thermal Condition is used to simulate prestressing force transfer.

4.3 Finite element sleeper model validation

In this step, the static capacity test of sleeper [**30**] is used to validate the material and structural properties of FE sleeper model. The simulation of time-dependent behaviour will be conducted when FE sleeper model has been validated. An experimental programme was conducted at Beijing Jiaotong University by Professor Jing's group. **Figure 4** shows the apparatus for this centre negative moment test of sleeper. The results of load-deflection responses for the prestressed concrete sleeper at centre, obtained from this experiment using digital image correlation (DIC), are utilised to evaluate the mesh sensitivity of FE model. The fracture results are used to validate the failure mode of the FE sleeper model.

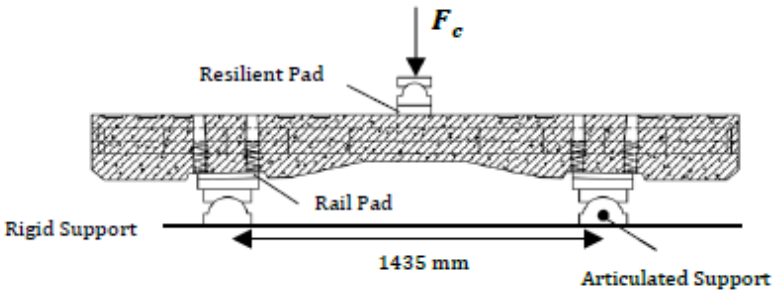

Figure 4. Apparatus of centre negative moment test of sleeper

4.3.1 Mesh size validation

In order to validate the FE prestressed concrete sleeper model, mesh sizes of 20mm, 30mm, and 40mm are attempted to use in sleeper model to analyse the mesh sensitivity. The results of load-deflection

responses (including experimental data and FEM) at the centre of prestressed concrete sleeper are plotted in **Figure 5**.

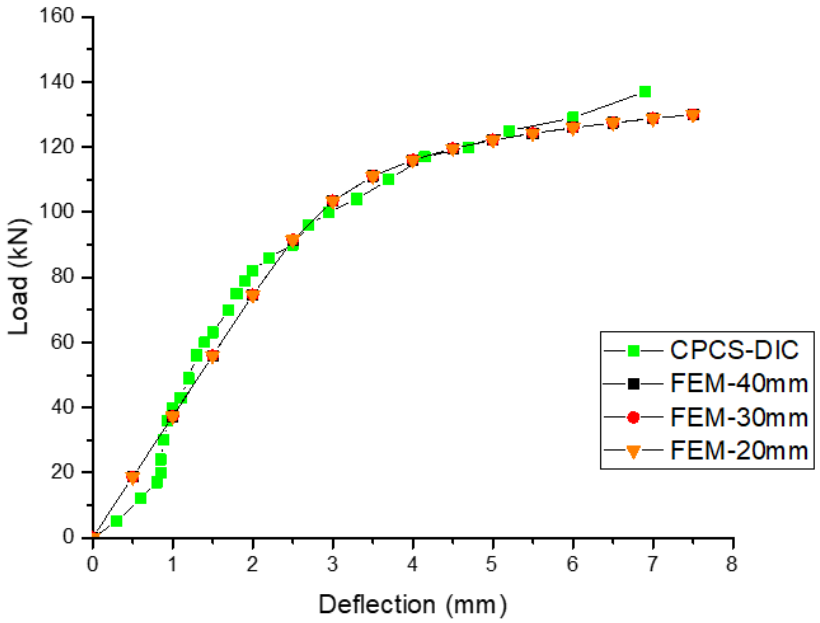

Figure 5. Load-deflection responses of prestressed concrete sleeper at rail centre section

Figure 5 shows the load-deflection responses between FEM 20mm, 30mm, and 40mm are slightly different. The 30mm mesh size is selected, in comparison with the DIC (experimental) results, this mesh size similar and close (with 5.99% max error). It can be seen that FE results accurately meets experimental data.

4.3.2 Failure mode validation

To complete the validation process, failure mode validation needs to be conducted. As we know, concrete starts cracking when the load exceeds maximum tensile strength. **Figure 6** shows *Normal Stress* distribution on the X axis of the FE model. In **Figure 6** the red area represents tensile zoom and the blue area is compressive zoom. With displacement increasing, the stresses also become larger. Once the X axis stress in tensile zoom reaches the tensile strength of the sleeper, it can be assumed to be cracking (failure). In this step, the tensile strength is calculated by the theoretical design standard (Eurocode 2) [**28**]. The tensile strength will be used for determining cracking load and deflection in FEM results in order to compare this with experimental cracking load/deflection. The mean value tensile strength of concrete f_{ctm} is given by:

$$f_{ctm} = 2.12 \ln(1.8 + 0.1 \times f_{ck}) \quad (14)$$

where f_{ck} is compressive strength of concrete.

The tensile strength is calculated as equal to 4.49 MPa, and the sleeper is assumed to start cracking after this point. The stress/load-deflection responses of mesh size 30mm FE model are illustrated in **Figure 7** in order to obtain cracking load. From **Figure 7**, the cracking deflection is 1.09mm when the X axis stress meets 4.49MPa. Therefore, the cracking load is 42.16kN. In the centre negative moment

test of the sleeper, the first cracking was observed at 45kN and from **Figure 5** (CPCS-DIC) the cracking deflection was at 1.13mm. The comparison between experimental and FE results is shown in **Table 5**.

	Experiment	**FE**					
		Size 20mm		***Size 30mm***		***Size 40mm***	
Cracking load	45kN	*kN*	*Deviation*	*kN*	*Deviation*	*kN*	*Deviation*
		42.12	6.39%	42.16	6.30%	42.03	6.61%

Table 5. Comparison cracking loads between experiment and FE

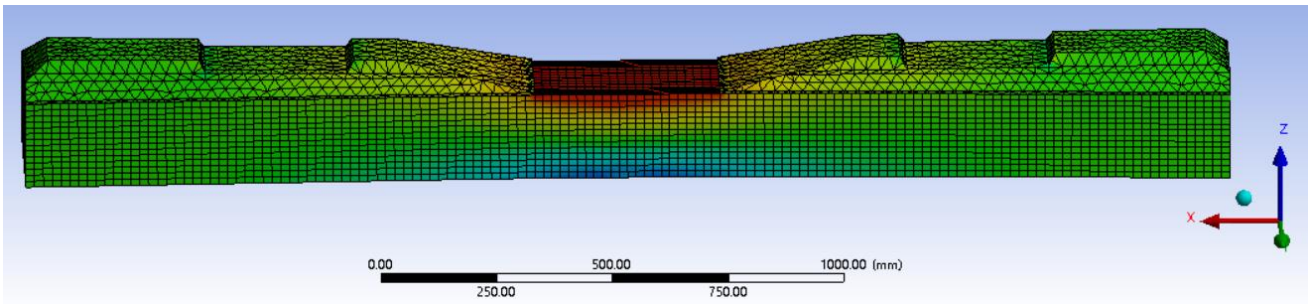

Figure 6. Normal stress distribution through X axis

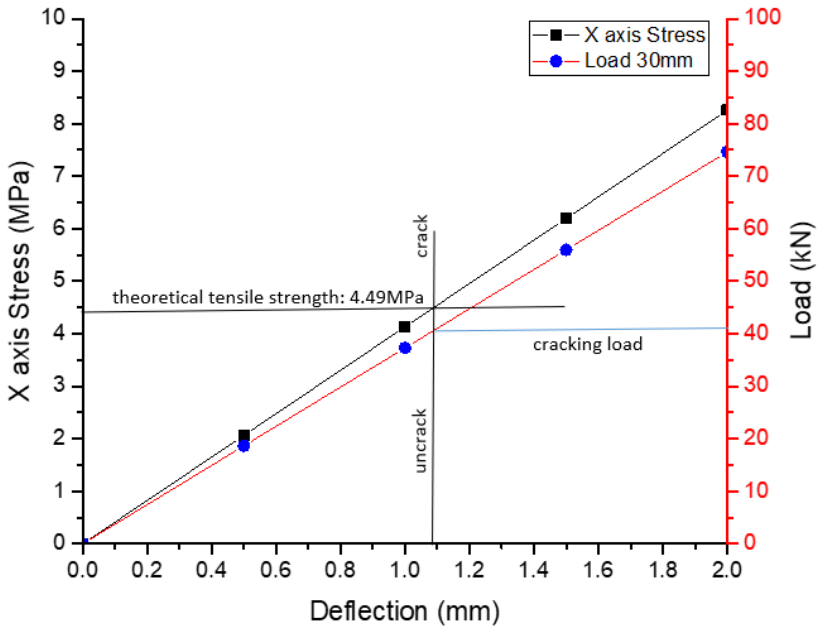

Figure 7. The stress/load-deflection responses of mesh size 30mm FE model

4.4 Analysis settings

4.4.1 Creep numerical model

In this study, the Creep Rate Equation is chosen to simulate the effect of creep. The equations consider the creep strain rate, which can be a function of stress, strain, temperature, and neutron flux level. The Time-hardening of *Creep Strain Rate Model* adopts the following functions:

$$\dot{\varepsilon}_{cr} = C_1 \sigma^{C_2} \varepsilon_{cr}^{C_3} e^{-C_4/T} \quad (15)$$

where:

$\dot{\varepsilon}_{cr}$ is change in equivalent creep strain with respect to time;

ε_{cr} is equivalent creep strain;

σ is equivalent stress;

T is temperature (absolute);

C_1, C_2, C_3, C_4 are constants.

The implicit method is used to analyse creep, which is robust, fast, accurate, and recommended for general use. The implicit method can model pure creep, creep with isotropic hardening plasticity, and creep with kinematic hardening plasticity, using both von Mises and Hill potentials. Where the material model combination with creep is supported, any of the implicit creep models can be used.

4.4.2 Shrinkage numerical model

Shrinkage consists of plastic shrinkage and drying shrinkage. Plastic shrinkage happens in the first few hours after placing concrete. Drying shrinkage is mainly due to loss of water by evaporation and this lasts perhaps for years after the prestressed concrete sleeper is put in service. Therefore, the shrinkage numerical model focuses on drying shrinkage simulation. The *Thermal Condition* are used in the shrinkage simulation. In this method, thermal deformation is used to predict time-dependent shrinkage shortening by changing temperature. The shrinkage shortening at specific time (in days) is converted to temperature. The prediction equation is shown below:

$$T = -250 + a * \exp(b * t) \quad (16)$$

where T is temperature that converts time-dependent shrinkage to thermal shortening;

t is time which unit in days;

a, b are constants.

5 Experiment

To evaluate the performance of prestressed concrete sleepers on time-dependent behaviour, an experiment was conducted at a concrete sleeper factory in Hebei province, China. Five Chinese Type III prestressed concrete sleepers were randomly selected since demoulding in sleeper factory. The sleepers were standard gauge which commonly used in ballasted railway in China. A series of static tests on the prestressed sleepers were performed in accordance with Eurocode 2. The average

compressive strength of demoulding concrete was 62MPa and the elastic modulus was 36500MPa. Each prestressing tendon with 7mm in diameter has a specified minimum proof force of 420kN.

To research deformation on prestressed concrete sleeper due to time-dependent behaviour, the critical dimension is measured so as to observe the change with time. This experiment lasted for 180 days. The setup for testing is illustrated in **Figure 8**. The distance between edge of rail seats is regarded as critical dimension which is 1818mm shown in **Figure 8**. In this investigation, the critical dimension measurement was arranged at 0, 7, 28, 35, 42, 49, 56, 60, 90, 180 days. The vernier calliper was utilised to conduct measurement. **Figure 9** shows critical dimension measurement of specimens conducted in sleeper factory. It should be noted that the measuring position for each specimen need to be marked in first measurement. This step guarantees the following testing would be carried out at same position to avoid human errors.

It should also be noted that the discreteness during the testing. Many influential factors could lead to the experimental results various. For example, in practice, the compressive strength and elastic modulus of concrete are varying with time. Even in same cuing conditions, the material properties could be different. The theoretical methods consider several main parameters and the value is constant. Environmental factor is the most difficult to control. The relative humidity measurement was also carried out which average value is approximate 70%. In fact, relative humidity could change every hour and it can also be affected by seasonal variation. Therefore, more than three specimens are suggested to test for average results.

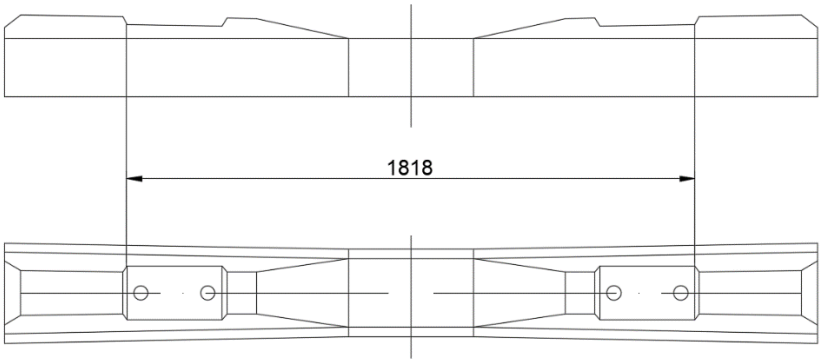

Figure 8. setup for time-dependent behaviour testing

Figure 9. Sleeper critical dimension measurement

6 Results and discussion

6.1 Theoretical results

The theoretical results were calculated for 40 years according to Eurocode 2 (the equation shown in Part 2). The information of material properties and sleeper structure were following Chinese Type III prestressed concrete sleeper details (shown in Part 3). The calculation of sleeper deformation was divided into two parts: centre and side. The length of centre sleeper is 400mm and both sides length is 709mm utilised to calculate the deformation. The width is determined by the cross-section of the sleeper. 75% relative humidity was applied in the theoretical calculation. The theoretical results of time-dependent behaviour are shown in **Table 6**.

Time	Creep	Shrinkage	Total shortening
(days)	***(mm)***	***(mm)***	***(mm)***
1	0.114	0.043	0.16
3	0.184	0.082	0.27
7	0.245	0.136	0.38
28	0.371	0.289	0.66
60	0.458	0.398	0.86
90	0.507	0.454	0.96
180	0.594	0.534	1.13
365	0.675	0.587	1.26
1095	0.766	0.626	1.39
1825	0.791	0.634	1.43
3650	0.814	0.640	1.45
7300	0.826	0.643	1.47
14600	0.832	0.644	1.48

Table 6. Theoretical results of time-dependent behaviour

6.2 Experimental results

The deformation between edges of rail seats were recorded for 180 days (shown in **Table 7**). The average deformation was also calculated in order to compare the theoretical and numerical results.

Time	X-1	X-2	X-3	X-4	X-5	Average
(days)	*(mm)*	*(mm)*	*(mm)*	*(mm)*	*(mm)*	*(mm)*
0	0	0	0	0	0	0
7	0.4	0.6	0.4	0.6	0.3	0.46
28	0.6	0.9	0.5	0.7	0.6	0.66
35	0.6	0.9	0.6	0.8	0.6	0.7
42	0.6	1	0.6	0.8	0.6	0.72
49	0.6	1.1	0.6	1	0.8	0.82
56	0.65	1.1	0.7	0.95	0.8	0.84
60	0.7	1.1	0.8	0.9	0.8	0.86
90	0.9	1	0.8	1.1	0.9	0.94
180	1.1	0.9	1	1.2	0.95	1.03

Table 7. Experimental results of time-dependent behaviour

6.3 Numerical results

The numerical models for time-dependent behaviour simulation were introduced in Part 4.4. The computation was carried out in Ansys Workbench. The time-dependent deformation, including creep and shrinkage, was respectively calculated for 10 years (3650 days) shown in **Table 8**.

Time	Creep	Shrinkage	Total shortening
(days)	*(mm)*	*(mm)*	*(mm)*
1	0.11439	0.01049	0.12488
3	0.18807	0.08915	0.27722
7	0.26182	0.12631	0.38813
28	0.3817	0.30038	0.68208
90	0.47508	0.42187	0.89695
180	0.53366	0.5257	1.05936
365	0.58838	0.54688	1.13526
1095	0.66287	0.58199	1.24486
3650	0.73918	0.61668	1.35586

Table 8. Numerical results of time-dependent behaviour

6.4 Discussion

Figure 10 shows a comparison between time-dependent deformation results of theoretical time-dependent behaviour prediction method and the numerical model for 10 years (3650 days). It is clear seen that both of creep and shrinkage increase with time. In early age, deformation increases sharply and after 3 years (1095 days) increasement of deformation becomes very slow. From **Figure 10**, the

deformation due to creep is higher than shrinkage, which creep has more effect on sleeper dimension than shrinkage. The results of the numerical models for both of creep and shrinkage can be compared against theoretical results on which the model is calibrated. The numerical models should at least be able to estimate time-dependent behaviour well. The maximum errors between theoretical and numerical results for creep and shrinkage deformation prediction are 13.46% and 7.03% respectively.

The 180-day experimental results are illustrated in **Figure 11** in order to validate FEM model and theoretical method. Experimental results present time-dependent deformation including creep and shrinkage. Therefore, theoretical and numerical results need to combine creep and shrinkage results in order to compare with experimental data. In **Figure 11**, both theoretical and numerical predictions are quite close to the experimental results while maximum errors for theoretical and numerical results in comparison with experimental data are 8.85% and 4.58% respectively. The comparison between the experimental and numerically obtained time-dependent deformation curves indicates that the numerical model is able to predict the development of time-dependent behaviour.

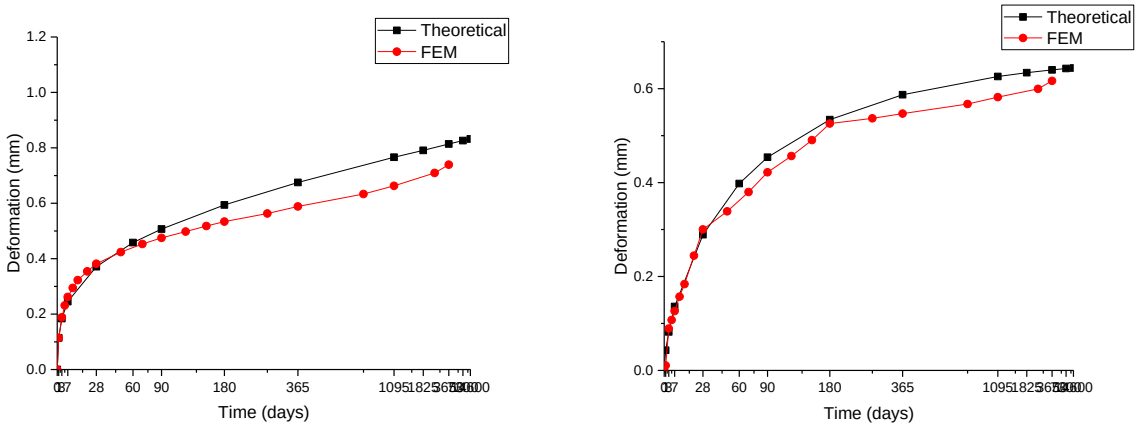

(a) creep deformation (b) shrinkage deformation

Figure 10. Comparison between theoretical and numerical results of creep and shrinkage for 10 years

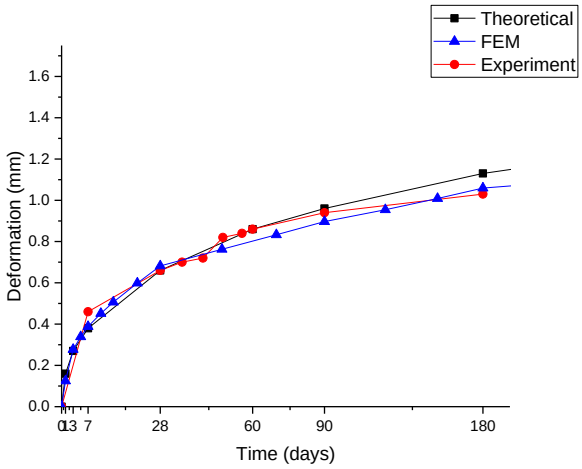

Figure 11. Comparison between theoretical, numerical and experimental results of time-dependent behaviour for 180-day

6.5 Parametric study

6.5.1 Concrete compressive strength

The material property is a key factor that influences time-dependent behaviour of prestressed concrete [**6**]. Therefore, various concrete compressive strengths of sleeper were studied to determine their performance. Based on the validated finite element model, concrete strengths of 45MPa, 55MPa, 65MPa, 75MPa, 85MPa are researched through a parametric study. The various concrete strength results are plotted in **Figure 12**. This figure compares deformation due to time-dependent behaviour with concrete compressive strength between 45MPa to 85MPa. It can be seen that the time-dependent behaviour, both of creep and shrinkage, is inversely proportional with the development of concrete strength. The results comply with theoretical predictions. From **Figure 12**, it can be seen that the maximum difference of time-dependent deformation between concrete strength 45MPa and 85Mpa is 0.574mm (42.3%). The deformation is reduced by almost 10% with concrete strength increasing to 10Mpa.

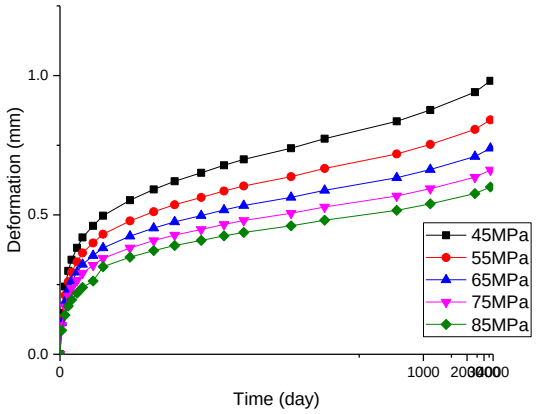

(a) creep deformation in various strength

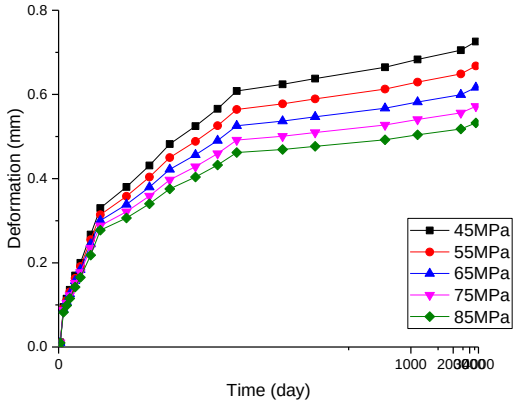

(b) shrinkage deformation in various strength

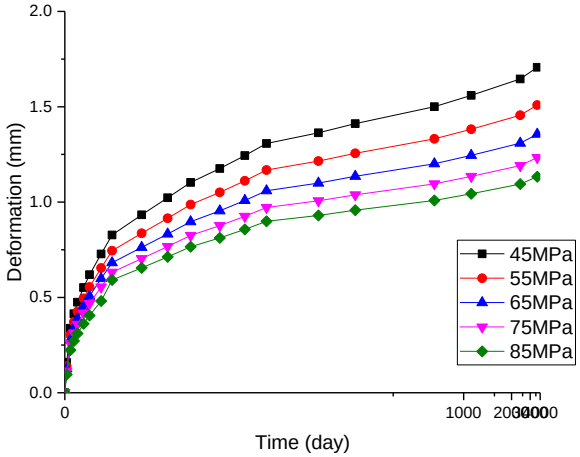

(c) total time-dependent deformation in various concrete strength

Figure 12. Parametric study of time-dependent behaviour in various concrete strength

6.5.2 Relative humidity

According to preview research, the most significant parameters affect creep and shrinkage are the concrete strength and relative humidity [**6**]. Therefore, the analysis of relative humidity is conducted. Based on the validated finite element model, the relative humidity of 50%, 60%, 70%, 80%, and 90% are studied. **Figure 13** illustrates the relationships between different relative humidity and time-dependent behaviour. This figure compares deformation due to time-dependent behaviour with relative humidity between 50% to 90%. It can be seen that the deformation tends to be higher when the relative humidity reduces. The difference of total deformation between 50% and 90% is up to 46.13%. In comparison creep and shrinkage deformation, creep has more influence by relative humidity. The difference of creep deformation between 50% and 90% is 53.74%, whereas the difference of shrinkage deformation is 39.19%. It is noted that the relative humidity is more likely to affect the performance of railway sleepers than concrete strength.

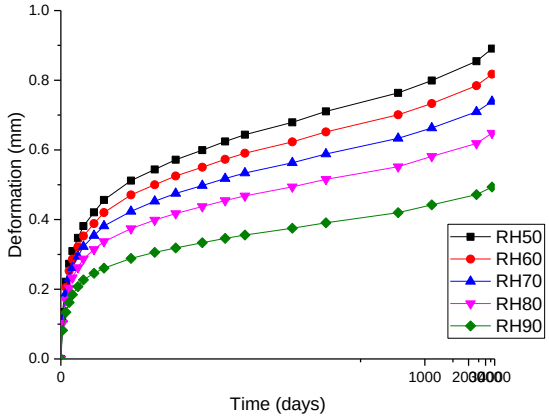

(a) creep deformation in various humidity

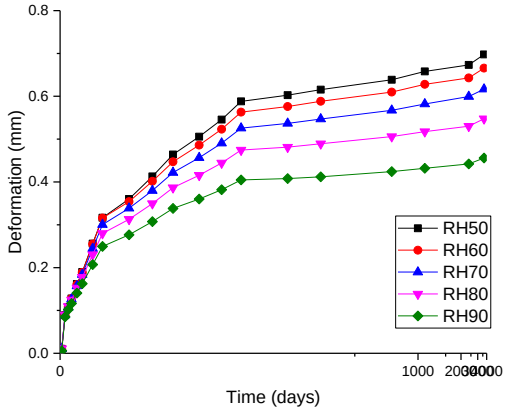

(b) shrinkage deformation in various humidity

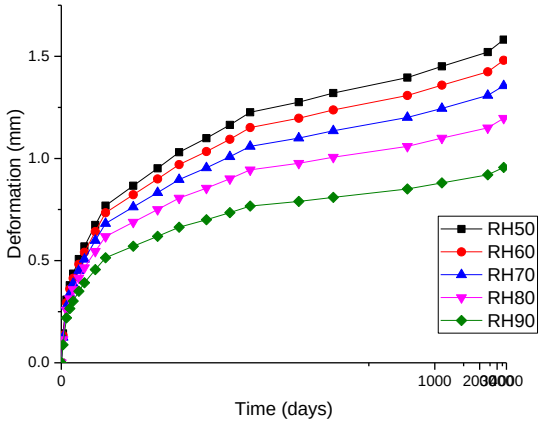

(c) total time-dependent deformation in various relative humidity

Figure 13. Parametric study of time-dependent behaviour in various relative humidity

6.5.3 Loss of prestress

Analysis of the long-term loss of prestress is an important part of the railway sleeper design process. In many prestressed concrete structures design process, the loss of prestress is a controlling parameter. The prestress loss could result in undesired deflections and cracking under service conditions. Loss of prestress occurs in two stages: loss at transfer and long-term loss. The immediate loss could be caused by anchorage, friction, and seating. The long-term loss is most due to interrelated effects of creep and shrinkage on concrete, and relaxation of steel tendons.

The Eurocode 2 [**29**] describes predict methods of loss due to time-dependent behaviour.

Loss due to creep: $Loss = \sigma_c \frac{E_s}{E_{cm}} \varphi$

Loss due to shrinkage: $Loss = \varepsilon_{cs} E_s A_{ps}$

Loss due to relaxation: $Loss = \Delta\sigma_{pr} A_{ps}$

The bottom part of midspan of the sleeper is selected as typical position to investigate the loss of prestress for numerical simulation (shown in **Figure 13**). The *Normal Stress* is used to checked the remained prestress in numerical model in different periods. The ratios of remained prestress and initial prestress are calculated in order to generate loss percentage. **Figure 14** illustrates the theoretical and numerical results of results of loss of prestress.

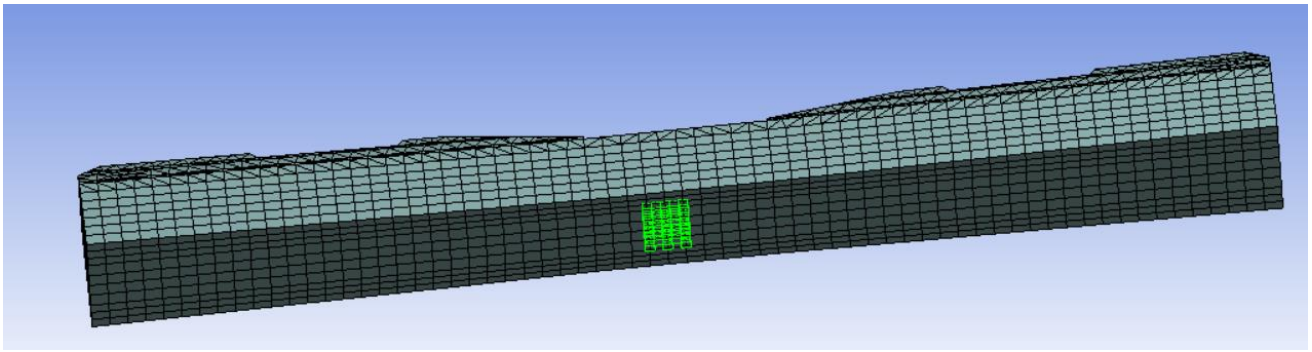

Figure 13. Typical position on numerical sleeper model for loss of prestress investigation

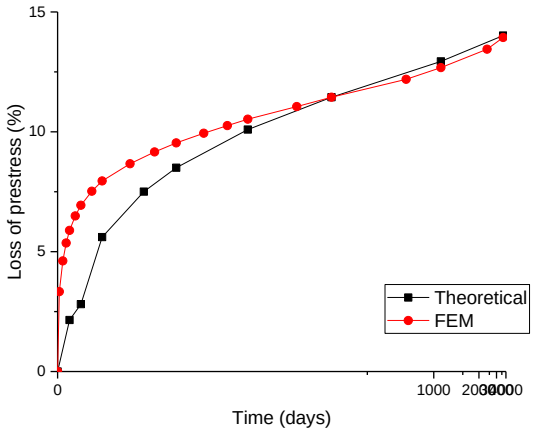

Figure 14. Comparison between theoretical and numerical results of loss of prestress

The numerical results comply with theoretical prediction. The loss of prestress exists along the whole life of railway sleepers. According to the experience of amount of preview research, the final value of remained prestress is only about 75% of the initial prestress [**31**]. In this study, the predicted loss of prestress is around 14%. The results can be used in further research to investigate the capacity of the railway sleeper.

7 Conclusion

Railway sleeper is one of the most important part in conventional track structure. Performance of prestressed concrete sleeper is influenced by time-dependent behaviour like other concrete structure. The deformation caused by creep and shrinkage can significantly influence the critical dimension of railway sleepers. Time-dependent behaviour of prestressed concrete sleepers is commonly related to material properties, environmental conditions, axle loads, and dynamic loads etc. A series of problems could be caused by time-dependent behaviour including dimension change, loss of prestress, cracks, deterioration, and decrease of capacity. The main effect of creep and shrinkage on railway sleeper happens in early-age service. First two months, the deformation due to time-dependent behaviour could reach 60% of total deformation. After 3 years, the deformation achieves 95% of total deformation and increasement becomes very slow and stable.

This paper presents the finite element results of Chinese Type III prestressed concrete sleeper analysis on the time-dependent behaviour. An experimental program was set up and completed where the critical dimension of five Chinese type III prestressed concrete sleepers were measured for 180 days in order to calibrate creep and shrinkage numerical models. This paper also introduces theoretical creep and shrinkage prediction methods based on Eurocode 2. The finite element model has been established and validated using comprehensive experimental data. The simulation shows great agreement in comparison with the theoretical and experimental results. The numerical results show that the creep and shrinkage deformation predicted by the numerical model are very close to 180-day experimental results. For 10-year prediction, numerical results are also very close to theoretical results which maximum error less than 13.46%. The relative humidity is also an important factor that influences creep and shrinkage. However, it is also very hard to control. In experiment, the relative humidity was not permanent during long-term measurement. It could be the reason that induces errors between experimental, theoretical, and numerical results.

In summary, for time-dependent behaviour, the relative humidity and concrete strength are the most influential factors. They largely influence creep and shrinkage. The parametric study highlights the effect of concrete strength, relative humidity, and loss of prestress. The parametric study indicates the increment of the concrete strength reduces time-dependent deformation and it provides a guide that railway engineer determines strength of sleeper when considering time-dependent behaviour. In addition, reduction of water-cement ratio will decrease time-dependent deformation. The environmental factors such as relative humidity needs to be considered comprehensively, because the relative humidity is more likely to affect the performance of railway sleepers than concrete strength. Dry climates usually result in more deformation due to creep and shrinkage. This opinion gives an instruction for railway sleepers serviced in harsh environments (dry climates area). In this situation, it is suggested that periodically sprays water on sleepers as maintenance in order to keep railway track moisture. The parametric study also reveals percentage of the prestress loss in different periods, which helps inspection of prestressed concrete sleepers in railway system.

In practice, the problems on prestressed concrete sleepers associated with time-dependent behaviour can be: (a) change of railway sleeper geometry and influence rail gauge; (b) Reduction of sleeper's loading capacity; (c) loss of prestress; (d) cracking on surface of railway sleepers. The major cause of these problems is due to creep and shrinkage. These problems could result in serious consequence like train derailment, increase of maintenance cost, service life of railway sleepers will reduce etc. It is necessary to investigate time-dependent behaviour and find a reliable method to estimate the potential effects on railway track system to avoid accidents. This paper presents the numerical analysis on time-dependent behaviour. It finds the main parameters affect time-dependent behaviour, and they are also applied in FE model to evaluate the performance of railway sleepers. The experimental results have a good agreement with numerical results that indicate the FE model is reliable. For the further research on creep and shrinkage, more parameters like load conditions, different materials, support conditions [**32-36**] will be reviewed to evaluate the performance of railway sleepers under various conditions.

This article proposes the reliability concepts and rationale associated with the development of time-dependent behaviour prediction methods. It reinforces the fundamental design guideline for prestressed concrete sleepers to optimally suit any local track. This paper addresses the importance challenge towards truly realistic condition-based predictive track maintenance. The outcome can be applied in long-term railway infrastructure maintenance, concrete manufacturer factory, design code. The insights will enhance the inspection of long-term serviced sleepers and improve track maintenance.

Acknowledge

The authors are grateful to Track engineering and Operations for Future Uncertainties (TOFU) Lab, University of Birmingham for support throughout this study. The authors would like to thank the Commission for H2020-MSCA-RISE, Project No. 691135 "RISEN: Rail Infrastructure Systems Engineering Network" (www.risen2rail.eu). Also, the first author wishes to thank the Tsinghua University, the China Academy of Railway Science (CARS) for the collaborative project. Valuable comments and support from Dr Ping Liu and Dr Chayut Ngamkhanong are acknowledged.

References

1. S. Kaewunruen, A.M. Remennikov, Impact capacity of railway prestressed concrete sleepers, Engineering Failure Analysis. 16 **(2009)** 1520–1532.
2. R. You, D. Li, C. Ngamkhanong, R. Janeliukstis, S. Kaewunruen, Fatigue Life Assessment Method for Prestressed concrete sleepers, Frontiers in Built Environment. 3 **(2017)** 1–13.
3. C. Ngamkhanong, D. Li, S. Kaewunruen, Impact capacity reduction in railway prestressed concrete sleepers with vertical holes, IOP Conference Series: Materials. **(2017)**.
4. S. Kaewunruen, C. Ngamkhanong, P. Sengsri, M. Ishida, On Hogging Bending Test Specifications of Railway Composite Sleepers and Bearers. Frontiers in Built Environment. 6 **(2020)**.
5. P, Liu, S, Kaewunruen, D, Zhao, S, Wang, Investigation of the Dynamic Buckling of Spherical Shell Structures Due to Subsea Collisions, Applied sciences. 8(7) **(2018)** 1148-52.
6. D. Li, S. Kaewunruen, P, Robery, A.M. Remennikov, Parametric studies into creep and shrinkage characteristics in railway prestressed concrete sleepers. Frontiers in Built Environment. 6 **(2020)** 130.
7. P, Liu, S, Kaewunruen, B, Tang, Dynamic Pressure Analysis of Hemispherical Shell Vibrating in Unbounded Compressible Fluid, Applied sciences. 8(10) **(2018)** 1938-42.
8. D. Li, S. Kaewunruen, Mechanical properties of concrete with recycled composite and plastic aggregates. International Journal of GEOMATE. 17 (60) **(2019)** 231-38.
9. D. Li, S. Kaewunruen, P. Robery, A.M. Remennikov, Creep and Shrinkage Effects on Railway Prestressed Concrete Sleepers. ICRT 2017: Railway Development, Operations, and Maintenance. **(2018)** 394-405.
10. P. Liu, S. Kaewunruen, B. Tang, Dynamic Pressure Analysis of Hemispherical Shell Vibrating in Unbounded Compressible Fluid, Applied sciences. 8(10) **(2018)** 1938-42.
11. X. Huang, J. Ge, S. Kaewunruen, Q. Su. The Self-Sealing Capacity of Environmentally Friendly, Highly Damped, Fibre-Reinforced Concrete Materials. 13(2) **(2020)** 298.
12. G. Q. Jing, P. Aela, H. Fu, M. Esmaeili, Numerical and Experimental Analysis of Lateral Resistance of Biblock Sleeper on Ballasted Tracks. International Journal of Geomechanics, 20(6) **(2020)**.
13. R. Janeliukstis, S. Ručevskis, S. Kaewunruen, Mode shape curvature squares method for crack detection in railway prestressed concrete sleepers, Engineering Failure Analysis. 105 **(2019)** 386-401.
14. J. Sadeghi, P. Barati. Comparisons of the mechanical properties of timber, steel and concrete sleepers, Structure and Infrastructure Engineering 8 **(2012)**.
15. C. Ngamkhanong, S. Kaewunruen, Influence of prestress losses on the dynamic over static capacity ratios of railway concrete sleepers, in SynerCrete'18 International Conference on Interdisciplinary Approaches, RILEM Publications S.A.R.L., Paris France. **(2018)** 925-30.
16. S. Kaewunruen, C. Ngamkhanong, J. Ng, Influence of time-dependent material degradation on life cycle serviceability of interspersed railway tracks due to moving train loads, Engineering Structures. 199 **(2019)**.
17. R. You, K. Goto, C. Ngamkhanong, S. Kaewunruen, Nonlinear finite element analysis for structural capacity of railway prestressed concrete sleepers with rail seat abrasion, Engineering Failure Analysis. 95 **(2019)** 47-65.
18. C. Ngamkhanong, D. Li, A Remennikov, S. Kaewunruen, Capacity reduction in railway prestressed concrete sleepers due to dynamic abrasions, 15th East-Asia Pacific Conference on Structural Engineering and Construction. **(2017)**.
19. C. Ngamkhanong, D. Li, A.M. Remennikov, S. Kaewunruen, Dynamic Capacity Reduction of Railway Prestressed Concrete Sleepers due to Surface Abrasions Considering the Effects of

Strain Rate and Prestressing Losses. International Journal of Structural Stability and Dynamics, 19(1) **(2019)**.

20. D. Li, S. Kaewunruen, Robery, P, Early-age responses of railway prestressed concrete sleepers to creep and shrinkage, in Proceedings of the 2nd International RILEM/COST Conference on Early Age Cracking and Serviceability. **(2018)** 567-72.
21. A. M. Remennikov, M. H. Murray, S. Kaewunruen, Reliability-based conversion of a structural design code for railway prestressed concrete sleepers, Journal of Rail and Rapid Transit. 226(2) **(2011)** 155-73.
22. W. Ferdous, A. Manalo, Failures of mainline railway sleepers and suggested remedies – Review of current practice, Engineering Failure Analysis. 44 **(2014)** 17-35.
23. J. Sadeghi. Field investigation on dynamics of railway track pre-stressed concrete sleepers" Advances in Structural Engineering 13.1 **(2010)**.
24. J. Sadeghi, P. Barati. Experimental evaluation of accuracy of current practices in analysis and design of railway track sleepers, Canadian Journal of Civil Engineering 35.9 **(2008)**.
25. D. Li, S. Kaewunruen, Effect of Extreme Climate on Topology of Railway Prestressed Concrete Sleepers, Climate. 7(1) **(2019)** 17.
26. W. He. Creep and Shrinkage of High-Performance Concrete and Prediction of Long-Term Camber of Prestressed Bridge Girders, Iowa State University. 2013.
27. K. A. Byle, H. Burns, R. Carrasquillo. Time-dependent deformation behaviour of prestressed high-performance concrete bridge beams. The University of Texas at Austin. 1997.
28. M. Lopez. Creep and shrinkage of high-performance lightweight concrete: A multi-scale investigation. Georgia Institute of Technology, 2005.
29. EN1992-2. Design of concrete structures. Part 2: concrete bridges design and detailing rules. Brussels; European Committee for standardization, 2005.
30. E. C. f. Standardization, Railway applications-track-concrete sleepers and bearers part 2: Prestressed monoblock sleepers, 2009.
31. P. Bhatt. Prestressed concrete design to Eurocodes, first edn., Abington: Spon Press (UK), 2011.
32. J. A. Zakeri, J. Sadeghi. Field investigation on load distribution and deflections of railway track sleepers[J]. Journal of Mechanical Science and Technology, 21(12) **(2007)**: 1948.
33. J. Sadeghi, A. R. Tolou Kian, and A. Shater Khabbazi. Improvement of mechanical properties of railway track concrete sleepers using steel fibres. Journal of Materials in Civil Engineering 28.11 (2016): 04016131.
34. S. Kaewunruen, and A. M. Remennikov. Investigation of free vibrations of voided concrete sleepers in railway track system. Proceedings of the Institution of Mechanical Engineers, Part F: Journal of Rail and Rapid Transit 221.4 **(2007)**: 495-507.
35. Taherinezhad, J., Sofi, M., Mendis, P. A., and Ngo, T. A Review of Behaviour of Prestressed Concrete Sleepers, Electronic Journal of Structural Engineering, 13(2): 1-16, (2013).
36. Kaewunruen, S., Ngamkhanong, C., Lim, C.H., Damage and failure modes of railway prestressed concrete sleepers with holes/web openings subject to impact loading conditions, Engineering Structures, 176, 840-848, (2018). doi:10.1016/j.engstruct.2018.09.057